

ARTICLES

Tailoring Porphyrins and Chlorins for Self-Assembly in Biomimetic Artificial Antenna Systems

TEODOR SILVIU BALABAN*

Forschungszentrum Karlsruhe, Institute for Nanotechnology, Postfach 3640, D-76021 Karlsruhe, Germany, and Center for Functional Nanostructures, University of Karlsruhe

Received June 16, 2004

ABSTRACT

There is much diversity in the way in which photosynthetic organisms harvest sunlight. In chromophore–protein complexes, an exact orientation of pigments by the protein matrix ensures an efficient stepwise energy transfer to the reaction center where charge separation occurs. The charge separation and subsequent electron transfer steps are, however, very similar in all organisms, proving that there must exist a common ancestor. The architectural principle of chromophore–protein complexes is too complicated to be replicated in artificial light-harvesting devices. A simpler principle employs self-assembling chromophores that early green photosynthetic bacteria use in their chlorosomal antenna systems. Efforts in mimicking this self-assembly algorithm with fully synthetic pigments are presented. The fact that, as in the natural system, after self-assembly, concentration quenching is not operating due to the very orderly manner in which the chromophores are positioned lends hope for applications in artificial devices, such as hybrid solar cells.

Introduction

Light-harvesting is the first step in a complex succession of energy and electron transfer events that make photosynthesis possible on Earth. Undisputable photosynthesis, either directly through organisms that convert light energy into biochemical energy or indirectly by incorporating such phototrophs into the food chain, is essential for life and is responsible for the present oxygen-containing, life-friendly atmosphere. The fact that dinosaurs became extinct might have been caused by the fact that light-harvesting was temporarily inhibited by a catastrophic event, such as a meteorite impact, or a volcanic eruption, leading to dust and debris clouds, which could have blocked sunshine for an extended period of time.¹ However, one may argue whether light capture is or is not the

most important elementary photosynthetic process, which has been carefully optimized during eons of evolution. It certainly accounts for the vast majority of pigments that are synthesized by plants, algae, and photosynthetic bacteria.

There is much diversity in conditions under which photosynthetic organisms have evolved light-harvesting apparatus or antennas. Thus, green sulfur bacteria, which live for example in the Black Sea at depths of over 50 m and still can capture sunlight of minute intensities, have a specialized antenna organelle, called the chlorosome (or green sac), which is also common to other filamentous, nonsulfur green bacteria.^{1,2} Near the water surface, where different illumination conditions are encountered, algae, cyanobacteria, and purple bacteria all have very different light-harvesting pigment–protein complexes. These in turn differ in their architecture, but not function, from those of terrestrial ferns and plants. By adapting to different habitats with widely different illuminations, photosynthetic organisms have been obliged to develop different solutions to light-harvesting. This is in stark contrast to the way in which light energy is actually converted into biochemical energy within the reaction centers, a feature carefully conserved during evolution. Within the reaction center (RC) protein complexes, very few specialized (bacterio)chlorophyll [(B)Chl] molecules, after electronic excitation energy transfer (EET) from the bulk antenna pigments, perform light-induced charge separation followed by successive electron transfer (eT) steps. Charge recombination is cleverly retarded so that eventually the hole and electron are separated on opposite sides of the photosynthetic membrane. This allows for protons to be pumped against a gradient. These protons in turn drive the ATP synthase, which forms an energy-rich phosphate bond, producing during oxygenic photosynthesis same reductant NADPH that the cells can then use to drive uphill endoergonic biochemical transformations. By solving the crystal structures of the two photosystems expressed in the cyanobacterium *Synechococcus elongatus*,^{3,4} it was only recently proven that the same overall architecture of RCs exists. Although slight differences exist, the same type of RC is common for all photosynthetic organisms, either bacterial or plants, proving that they must have a common ancestor. In other words, any organisms with other eT chains are presently not known and have probably not survived.

Can we learn something from the diversity of the natural light-harvesting systems in order to engineer artificial antenna systems? These should allow not only coupling to reaction centers but also might be used in hybrid solar cells that could operate under low or moderate illumination conditions. At present, silicon-based solar cells represent a functioning technology and have achieved

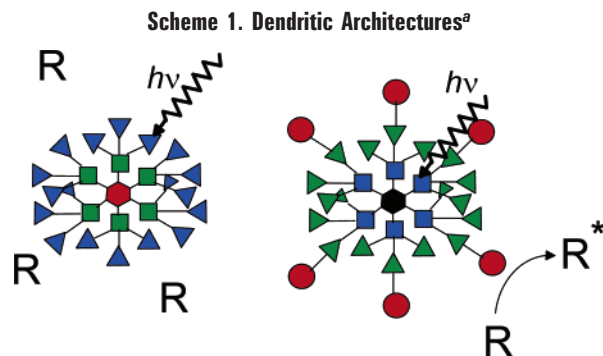
Silviu Balaban was born in Bucharest, Romania, and obtained a chemical engineering degree and a Ph.D. in organic chemistry under the supervision of the late Ecaterina Cioranescu-Nenitzescu from the Bucharest University "Politehnica". Postdoctoral studies in Germany were due to an Alexander von Humboldt Fellowship, followed by a Max-Planck-Society Fellowship, with the late Günther Snatzke (Bochum), Klaus Hafner (Darmstadt), and Kurt Schaffner at the Max-Planck Institute for Radiation Chemistry (Mülheim/Ruhr). Following appointments in France with the CNRS (Strasbourg) and as Maître de Conférences at the Collège de France, Silviu moved back to Germany in 1999, to the Research Center in Karlsruhe, where he has set up a Supramolecular Chemistry Laboratory, in what is now the world's oldest Institute for Nanotechnology, where he holds a permanent research position. He has habilitated in 2000 in Strasbourg under the guidance of Jean-Marie Lehn.

* E-mail: silviu.balaban@int.fzk.de.

in industrially manufactured devices an incident photon-to-current conversion efficiency (IPCE) of $\sim 14\%$, but they still are too costly to allow large-scale applications, as the cost of $\sim \$1/\text{kW}\cdot\text{h}$ is 10 times higher than that of conventionally produced electric energy. However, these solar cells represent a very safe technology and are increasingly finding applications when price is not an issue, for example in space or along the highways for powering emergency telephones. The now emerging organic solar cells, which could be produced on large and flexible sheets using polymer technologies (with $>4.5\%$ IPCE) are still in their infancy, although their proof of principle has been demonstrated.⁵ A doubling of this IPCE value could lead to economically viable alternatives.

A legitimate question is, why use an antenna system when silicon solar cells or even reaction centers can be photoexcited directly to produce electron–hole pairs (excitons)? Nature teaches us that there are three good reasons to couple an antenna complex to a reaction center: (i) As with satellite dishes, the photon capture cross-section is markedly increased, a fact which leads to a stunning efficiency for energy trapping. Almost every photon captured by the antenna can eventually have its energy trapped, thus leading to useful charge separation with a quantum efficiency of almost unity (0.95–0.98 in some systems). (ii) The RC can be cycled much more rapidly. This means that during the time after charge separation, until the eT steps have been completed (on a nanosecond time scale, until the electron is recaptured), the reaction center remains “closed”, being thus unable to function; optimum cycling, sometimes even at 1 kHz, can be performed only with the aid of a large antenna system. (iii) A much broader wavelength range of solar radiation can be used for useful work. The antenna pigments, often due to inhomogeneous broadening, but also due to enrolling several different chromophores, have a much larger absorption range than the “special pair” of (B)Chls within RCs, which is responsible for the charge separation. Features i–iii ensure that photosynthetic organisms function properly also under diffuse and dim light. This is not the case with present state-of-the-art solar cells. If this were feasible, a lot of environmental problems related to current energy production, such as pollution due to radioactive waste disposal and greenhouse effects caused by the burning of fossil fuels, could be solved. Furthermore, solar energy conversion would not be restricted to high sunshine and low population density areas, but could be attained where energy consumption is needed, avoiding thus energy storage and transportation issues.

The architectural principle of chromophore–protein (CP) complexes is much too complicated to be replicated in artificial light-harvesting devices. The few synthetic peptides that have been engineered for chromophore binding or the recombinant proteins with synthetic chromophores, especially related to eT studies,⁶ have proven that it is not yet feasible to reproduce synthetically Nature’s most successful architectural principle of CPs for light-harvesting. Elegant synthetic routes to complicated



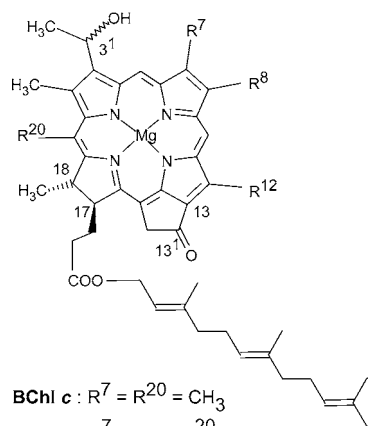
^a At left is depicted a dendrimer with a red-shifted core that acts as an energy trap but to which access is sterically blocked. At right, the inverse architecture is shown that allows photosensitization of a reactant R.

covalent light-harvesting arrays have been developed by several groups, among which Lindsey’s^{7,8} and Gossauer’s^{9,10} achievements deserve special mention. However, the covalent, bond-by-bond construction of nanostructures that should act as efficient antennas encompassing say a hundred chromophores per RC is not (yet) practicable. One feasible covalent approach is to construct dendrimers using repetitive, high-yielding reaction sequences, to access successive generations of light-harvesting units. The groups of Fréchet,^{11,12} Aida,¹³ and Müllen¹⁴ are championing this field. One problem associated with the dendrimeric architecture is that the vectorial energy transfer from the “blue” to “red” chromophores in most architectures synthesized so far occur from the periphery toward the dendrimer’s core (Scheme 1). Efficient trapping indeed could be proven in several ingenious constructs. However, if practical applications are envisaged, energy trapping within the core is useless, as access of other reactants is sterically blocked and only thermal deactivation can occur beside the undesired charge recombination. Aida’s example of a *cis*–*trans*-azobenzene isomerization using an IR antenna clearly demonstrates this.¹³ An inverse dendrimeric energy flow, as implied in Scheme 1, from a blue-shifted core toward the more and more red-shifted periphery, where eventually the energy can be trapped within one single artificial RC, has not been realized so far. Attempts to self-assemble dendritic chromophore architectures onto silicon wafers, which show interchromophore EET, have been successful.^{11,15}

A synthetically much less demanding task is to use as in the chlorosomes self-assembling chromophores. Self-assembly, when correctly programmed, can lead to large functional nanostructures, thus being a key principle that might work in a nanotechnological approach to light-harvesting. This Account summarizes some of our efforts in equipping synthetic chromophores with groups that under appropriate conditions induce self-assembly. Our approach to light-harvesting is thus biomimetic as in the chlorosomal antennae.

Self-Assembly of Chromophores into Functional Antennas

Before oxygenic photosynthesis evolved, ancient organisms were forced to a stringent economy both in bio-

Chart 1. Natural BChls Encountered in Chlorosomes^a

BChl c: $R^7 = R^{20} = \text{CH}_3$

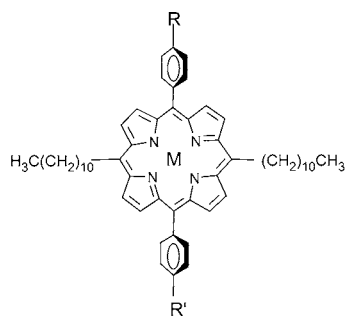
BChl d: $R^7 = \text{CH}_3$; $R^{20} = \text{H}$

BChl e: $R^7 = \text{CHO}$; $R^{20} = \text{CH}_3$

^a Farnesol is the fatty alcohol shown to esterify the 17-propionic acid residue. Also encountered in BChls are stearol, cetol, phytol, geranylgeraniol, etc. The R^8 substituent of BChls can be either methyl, ethyl, propyl, isobutyl, or neopentyl, while the R^{12} substituent can be methyl or ethyl. Note that both 3¹ (*R*)- and (*S*)-epimers are encountered for various homologues.

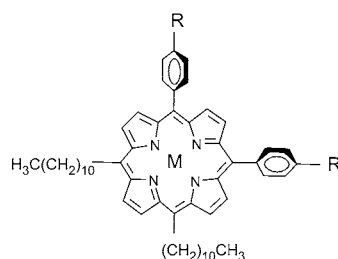
chemical processes and in genes. One ingenious solution for constructing large antenna systems, which as mentioned in the beginning can still harvest very dim light, was to construct chromophoric building blocks able under appropriate conditions to self-assemble into large, functional structures. Viruses are yet another example where

self-assembly is mastered at the border between living and inanimate matter. Green photosynthetic bacteria evolved a unique organelle, the chlorosome, which agglomerates BChl *c*, *d*, or *e* molecules (Chart 1). The most intriguing feature is that concentration quenching does not operate among the pigments, so they act collectively, passing on the radiant energy to traps located on the inner side of the cytoplasmic membrane, very close to where the RCs are embedded. Large delocalization distances have been measured for excitons within the chlorosomal “rods”, structural elements put into evidence by early freeze-fracture microscopy studies.^{16,17} These nanorods, as one would obviously call them today, are 4–5 nm in diameter and have lengths of up to several hundred nanometers and exist in a very hydrophobic environment staged by encirclement with a monolayer lipid membrane. Although initially debated, it is now generally accepted that the BChls self-assemble within these nanorods without the aid of proteins as in CPs. Several reviews have appeared,^{1,2} but there is yet no crystallographic proof for the chlorosome architecture, making room for several models on the details of the self-assembly mechanism to be more or less controversially discussed. From solid-state NMR spectra on ¹³C-labeled BChl *c*, both within chlorosomes and after induced self-assembly, it became clear that the BChl molecules form a π -stacked structure.¹⁸ The circular structure put forward by Holzwarth and Schaffner on the

Chart 2. Self-Assembling Porphyrins and Chlorins^a

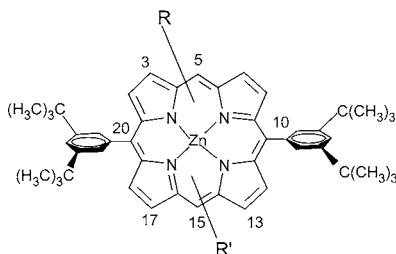
1: $R = R' = \text{CH}_2\text{OH}$, $M = 2\text{H}$

2: $R = \text{CH}_2\text{OH}$; $R' = \text{CHO}$, $M = \text{Zn}$



3: $R = R' = \text{CH}_2\text{OH}$, $M = 2\text{H}$

4: $R = \text{CH}_2\text{OH}$; $R' = \text{CHO}$, $M = \text{Zn}$



5: $R = 5\text{-CH(OH)-CH}_3$; $R' = 15\text{-COCH}_3$

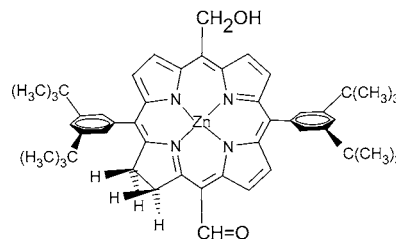
6: $R = 3\text{-CH(OH)-CH}_3$; $R' = 13\text{-COCH}_3$

7: $R = 5\text{-CH}_2\text{OH}$; $R' = 13\text{-COCH}_3$

8: $R = 3\text{-CH(OH)-CH}_3$; $R' = 15\text{-CHO}$

9: $R = 5\text{-CH}_2\text{OH}$; $R' = 15\text{-CHO}$

10: $R = 3\text{-CH(OH)-CH}_3$; $R' = 17\text{-COCH}_3$



11

^a Zn-porphyrins **2** and **4** (formed from **1** and **3**, respectively, by mono-oxidation and zinc metalation) did not give chlorosomal self-assembly,²³ while our later constructs **5–11** did self-assemble, being thus the first fully synthetic perfect mimics of the natural BChls *c*, *d*, and *e*.^{24–26} Note that the numbering of the porphyrins was proposed to follow the one used for (B)Chls so that the hydroxy(m)ethyl substituents are in the northern half of the molecule, while the carbonyl groups are in the southern half.

basis of a molecular modeling study¹⁹ initially seemed to reconcile all spectroscopic evidence gathered so far.^{18,20} On the basis of further solid-state NMR work, a refined model was subsequently devised where concentric tubular structures accounted for additional sets of signals.²¹ Very recently, from studies on a Cd–BChl *d* analogue, further support for this model was presented.²²

We have taken a synthetic approach to the elucidation of the self-assembly mechanism responsible for the chlorosome structure by appending onto porphyrins the same or similar functional groups as in BChls *c*, *d*, and *e*. Porphyrins are more robust and more easily available than BChls and Chls, should applications become possible with artificial light-harvesting devices. Our synthetic concept is to use preformed porphyrins which have tailored groups for inducing solubility, such as undecyl²³ or 3,5-di-*tert*-butylphenyl groups,^{24–26} and then to further derivatize the porphyrins by means of high-yield reaction sequences for strategically positioning functional groups capable of inducing self-assembly. We were not initially successful, as our first porphyrins (**2** and **4** in Chart 2), although they had the same groups as BChl *c*, namely a hydroxy group, a carbonyl group, and zinc as a central metal atom, failed to self-assemble.²³ Only by solving the crystal structure of a precursor molecule, namely **1**, did it become evident that the desired self-assembly algorithm is inhibited to proceed, owing to steric hindrance due to the *meso*-phenyl substituents, which were therefore removed in future constructs. Several novel porphyrins (**5–10** in Chart 2) were then accessed, sometimes by devising novel reactions or by sequencing known reactions and protective group strategies.^{24–26} In all cases, when the self-assembly operates, red-shifted and broad absorption spectra are formed as in J-aggregates.^{27,28} Addition of minute but suprastoichiometric amounts of a solvent which competes for the metal ligation, in our case zinc, leads to complete disassembly of the large aggregates. These aggregates are a dynamic system: enthalpy wins over entropy so that aggregation proceeds until large structures (visible to the eye) flocculate from the solution. Shaking of the resulting suspension, due to shearing forces, leads to complete disappearance of the macroaggregates and to the formation of nanoaggregates with the same broad absorption spectra.^{24,29} Depending upon the concentration and temperature, after several minutes to hours, the macroaggregates reassemble. This behavior parallels exactly that of BChl *c* for which we could measure the kinetics of aggregation, and we could fit this to a model that resembles that of seeded crystallization.²⁹ Apparently a “critical nuclei” of ~14 BChl molecules is needed in order that new molecules become attached more rapidly than other ones can be disassembled, so that aggregate growth proceeds. High concentrations and low temperatures speed up the kinetics.

The synthetic strategy for accessing these BChl mimics used dicarbonyl compounds as intermediates. Selective monoreduction was possible as one carbonyl activates the other one so that the monoalcohols could be isolated in good yields. Protection of the more reactive formyl groups

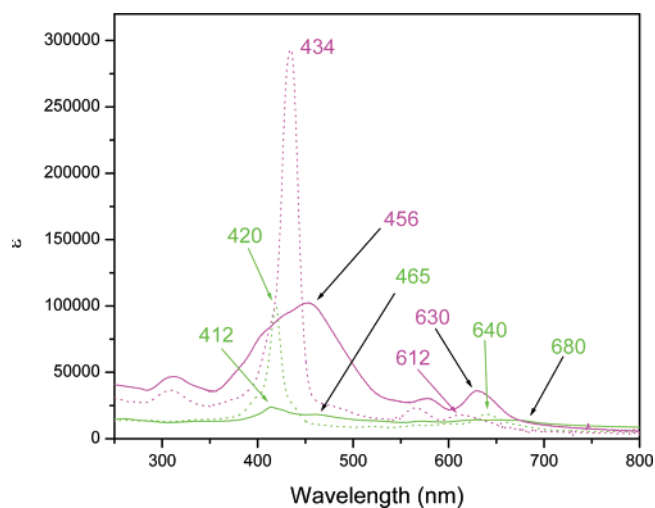
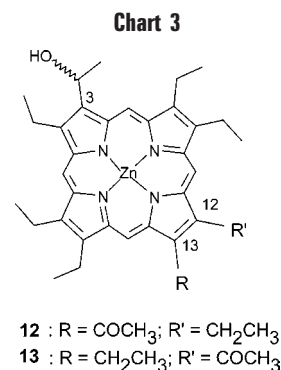


FIGURE 1. Typical absorption spectra of self-assembled porphyrin **7** (magenta full trace) and after disassembly with methanol (magenta dotted line) and the corresponding spectra of chlorin **11** (green traces). Aggregate maxima for the Soret and Q-bands (in nm) are indicated by black arrows.



allowed either monoreduction of acyl substituents (as for **8**) or transformation of the porphyrin into a chlorin (**11**).²⁵ Contrary to what we expected, the chlorin **11**, although it self-assembles in a manner similar to the other porphyrins and gives rise to broad absorption spectra, in its monomeric form does not have increased absorption coefficients in the visible range (the Q-bands) as compared to the porphyrins. Rather, the Soret band of the chlorin is decreased by a factor of ~3 in comparison to the porphyrins so that apparently the relative ratio of the Q-bands to the Soret band appears to be higher in chlorins (Figure 1). In the natural (B)Chls, the five-membered annulated ring that gives rise to the phorbins skeleton is an essential structural feature that is responsible for the high extinction coefficients in the visible region.²⁵

Tamiaki and co-workers, by using very elegant synthetic procedures, have also engineered the same groups that are responsible for the self-assembly in BChls onto octaethylporphyrins **12** and **13** (Chart 3).³⁰ It was very gratifying to see that similar broad absorption spectra were encountered with self-assembled **12** as in our systems **5–11**.^{24,25}

Very recently, we could solve the crystal structure of two crystal modifications of zinc porphyrin **5** (having a 5-hydroxyethyl and 15-acetyl groups) in a nonpolar en-

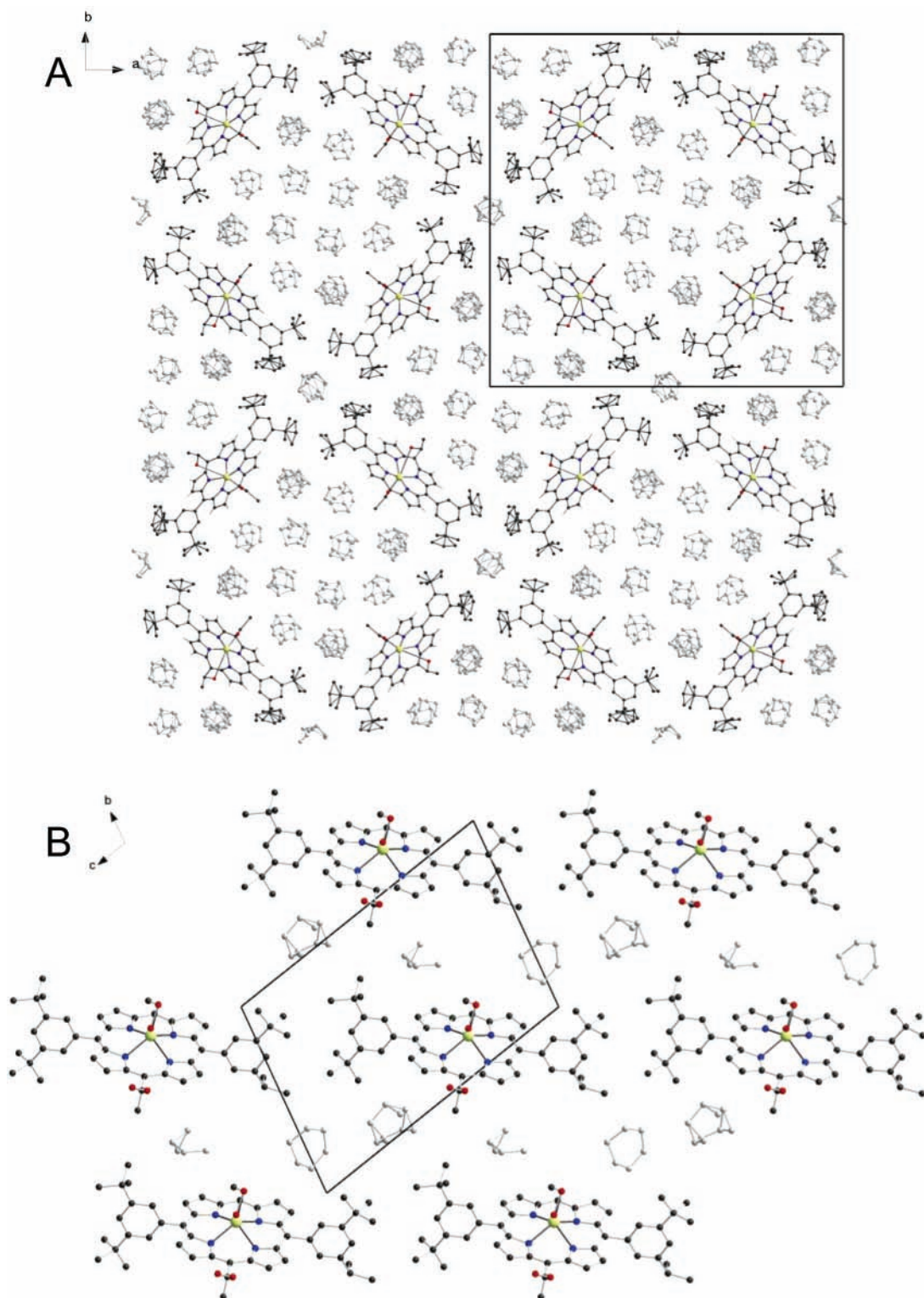


FIGURE 2. Two different crystal modifications of **5**. Due to statistical disorder, both the oxygen atoms (shown in red) and the carbon atoms of the solvent (cyclohexane, shown in gray) appear in multiple, partially occupied positions. The view is along the short crystallographic axis, perpendicular to the stacking direction. Reprinted with permission.

environment staged by cyclohexane.²⁶ At low concentrations, a crystal modification involving seven cyclohexane molecules per monomer and having a tetragonal symmetry was formed (Figure 2A). At higher concentrations, crystallization was somewhat more rapid, but much smaller crystals having three cyclohexane molecules per monomer

could be isolated (Figure 2B). The solving of the second crystal structure needed synchrotron radiation and was finally possible due to a fruitful collaboration between four crystallographers.²⁶ Both crystal modifications involve extended stacks of zinc porphyrins where the zinc atom is ligated by an oxygen atom from one side of the

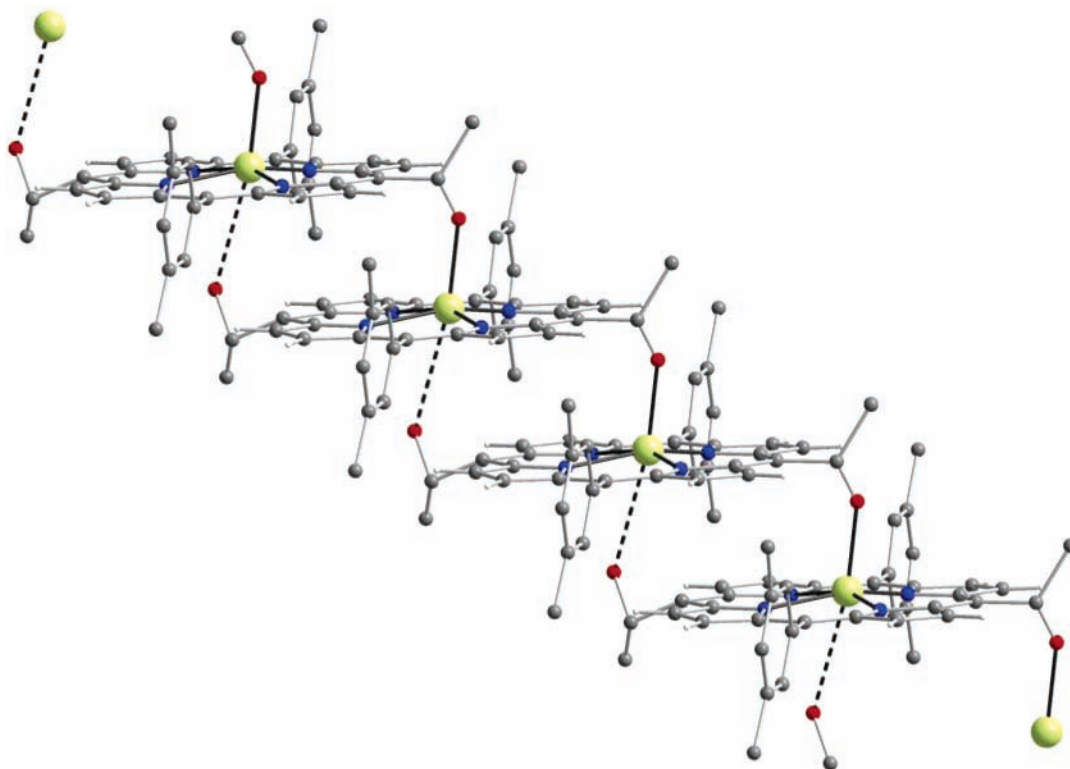


FIGURE 3. Stacks of **5** encountered in the two different crystal modifications. Shown here is an upward orientation with zinc (green), carbon (black), nitrogen (blue), and oxygen atoms as (red). Due to statistical disorder, both upward and downward stacks are encountered in the lattice. Long-range carbonyl–zinc interactions are shown with dotted lines. Reproduced with permission.

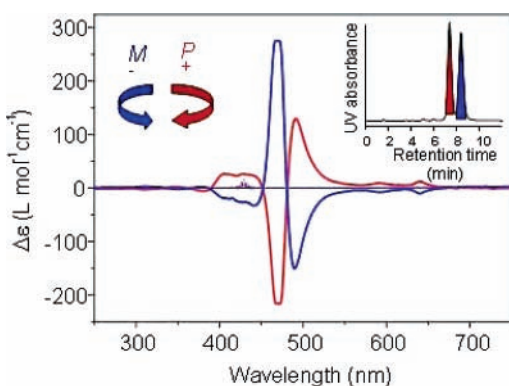


FIGURE 4. CD spectra of self-assembled **8**. Dotted lines superimposing the zero line are after disassembly with methanol. The M or P helicities of the self-assembled nanostructures can be assigned from the sign of the longest wavelength Cotton effect. Inset, typical chiral HPLC trace. Reproduced with permission from Wiley (VCH) (*Eur. J. Org. Chem.*).

porphyrin plane. Astonishingly, the opposite side is covered by a second oxygen atom of the acetyl group, which is twisted out of conjugation with the porphyrin macrocycle (Figure 3). This weak ligation (over 3.2 Å of the Zn–O distance) was the most surprising element revealed by these two crystal structures, and it explains very nicely why hydrogen bonding is absent between parallel stacks: there is no hydrogen-bond-accepting group available for the hydroxy group. The “busy” carbonyl group donates electron density to the zinc atom. This peculiar carbonyl group, at the expense of conjugation and loss of the green

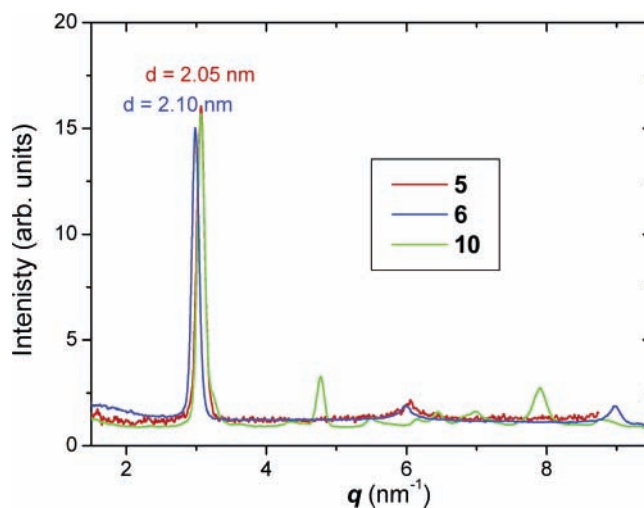


FIGURE 5. SAXS spectra of self-assembled BChl *c* mimics. Reproduced with permission.

color,²⁵ provides a fine-tuning element for staging other supramolecular interactions than hydrogen bonding. Thus, the cooperative oxygen–zinc ligation with extended π -stacking and numerous hydrophobic interactions between the bulky 3,5-di-*tert*-butylphenyl groups and the effect of the cyclohexane solvent, which cements together adjacent stacks, prevail over the putative hydrogen bonding.

The chirality of the 3-hydroxyethyl group in **5**, **6**, **8**, and **10** induces the chirality of the supramolecular self-assemblies. The enantiomers separated by chiral HPLC,

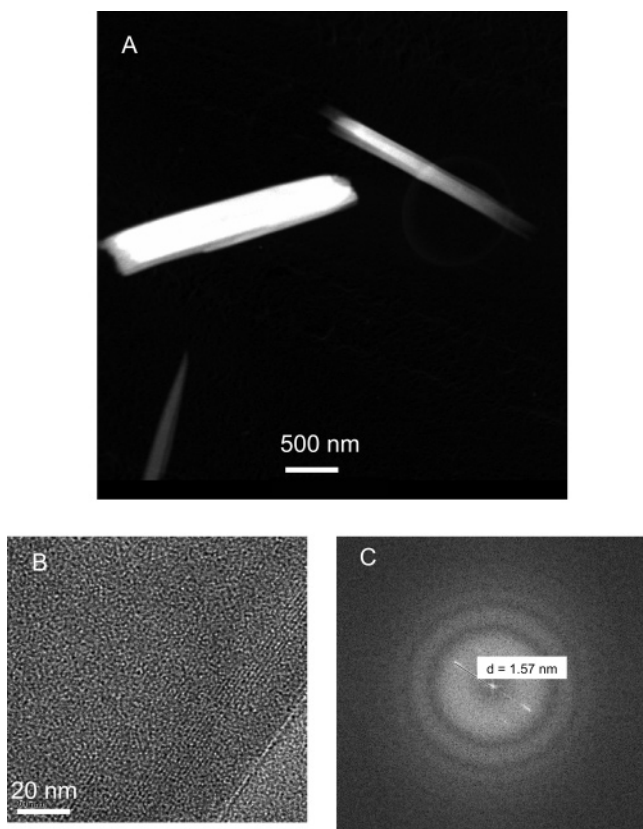


FIGURE 6. TEM of (*rac*)-**10**. (A) STEM overview. (B) HR-TEM from a portion in part A. (C) Fast Fourier transformation of the image in B showing reflexes at 1.57 nm. This spacing may vary depending on the compound, sample, and its orientation to the electron beam.

when induced to self-assemble, give rise to giant circular dichroism signals [also called *polymer* and *salt induced* (*psi*) type] consisting of excitonic couplets of opposite sign (Figure 4).^{24,25} Interestingly, the self-assembly proceeds much more easily with the racemates than with the separated enantiomers, as put into evidence by TEM and STEM images.²⁶ This provides an explanation to the long-standing question, why are both 3¹-epimers of BChls *c*, *d*, and *e* present within chlorosomes, when usually biosynthetic pathways lead to enantiopure compounds? Apparently, a heterochiral self-assembly is thermodynamically favored over the homochiral one. Molecular modeling supports this hypothesis.

Figure 2 shows the packing of the porphyrin stacks in the two crystal modifications with a view along the short crystallographic axis so that all the molecules within a stack appear superimposed. While the more dilute crystallization conditions have led to the tetragonal structure having cavities filled with crystallization solvent, the more concentrated solutions have led to a lamellar type structure with a long crystallographic axis of ~ 2 nm. This distance corresponds exactly to the Zn–Zn spacings and is responsible for a sharp and strong reflex in the small-angle X-ray scattering (SAXS) spectra not only of compound **5** but also of the isomeric ones **6** and **10** as shown in Figure 5. Furthermore, high-resolution transmission

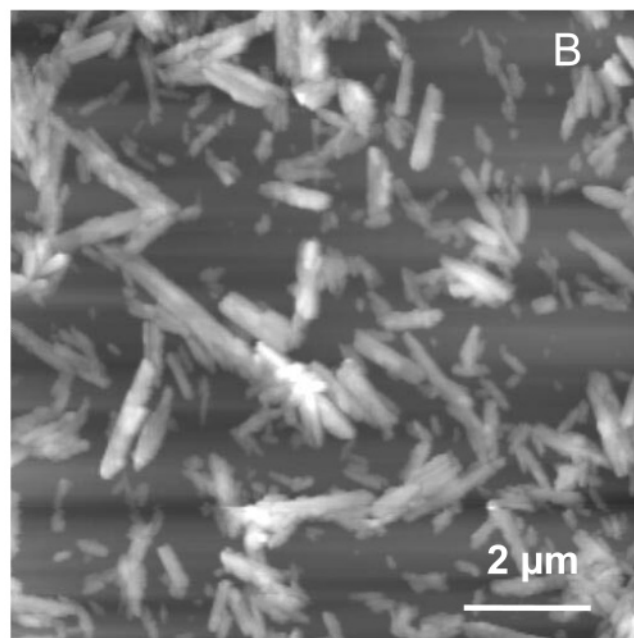
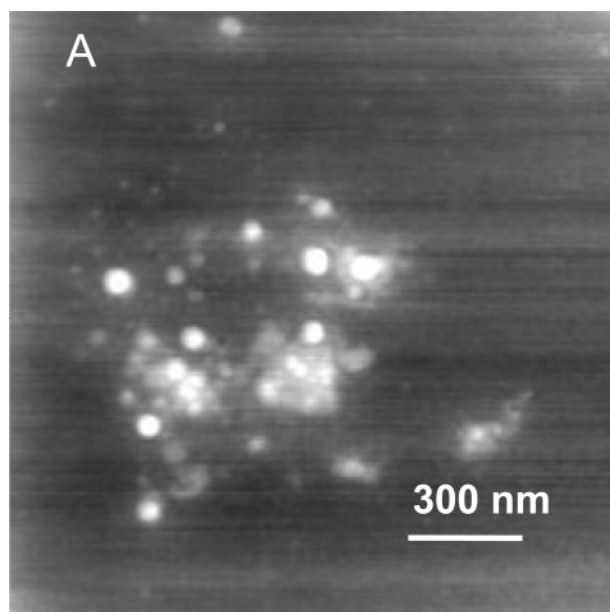


FIGURE 7. AFM images: (A) achiral **7**; scan area, $1.5 \mu\text{m} \times 1.5 \mu\text{m}$; z-range, 100 nm; (B) (*rac*)-**6**; scan area, $10 \mu\text{m} \times 10 \mu\text{m}$; z-range, 300 nm. Note the tubular aspect and the large size distribution in image B. Reprinted with permission from Wiley-VCH.

electron microscopy (HR-TEM) images of several of our self-assemblies show parallel striations with spacings that depend on the orientation of the sample to the electron beam ranging from 1.5 to 2.1 nm. (Figure 6).

Both atomic force microscopy (AFM) and scanning TEM (STEM) images show a relatively broad size distribution of the aggregates. Interestingly, in the case of the racemic compounds **5**, **6**, **8**, and **10**, tubular structures with a high aspect ratio are encountered, very similar to the natural chlorosomes. In the case of the achiral hydroxymethyl substituent (**7**, **9**), however, only globular superstructures were encountered (Figure 7).

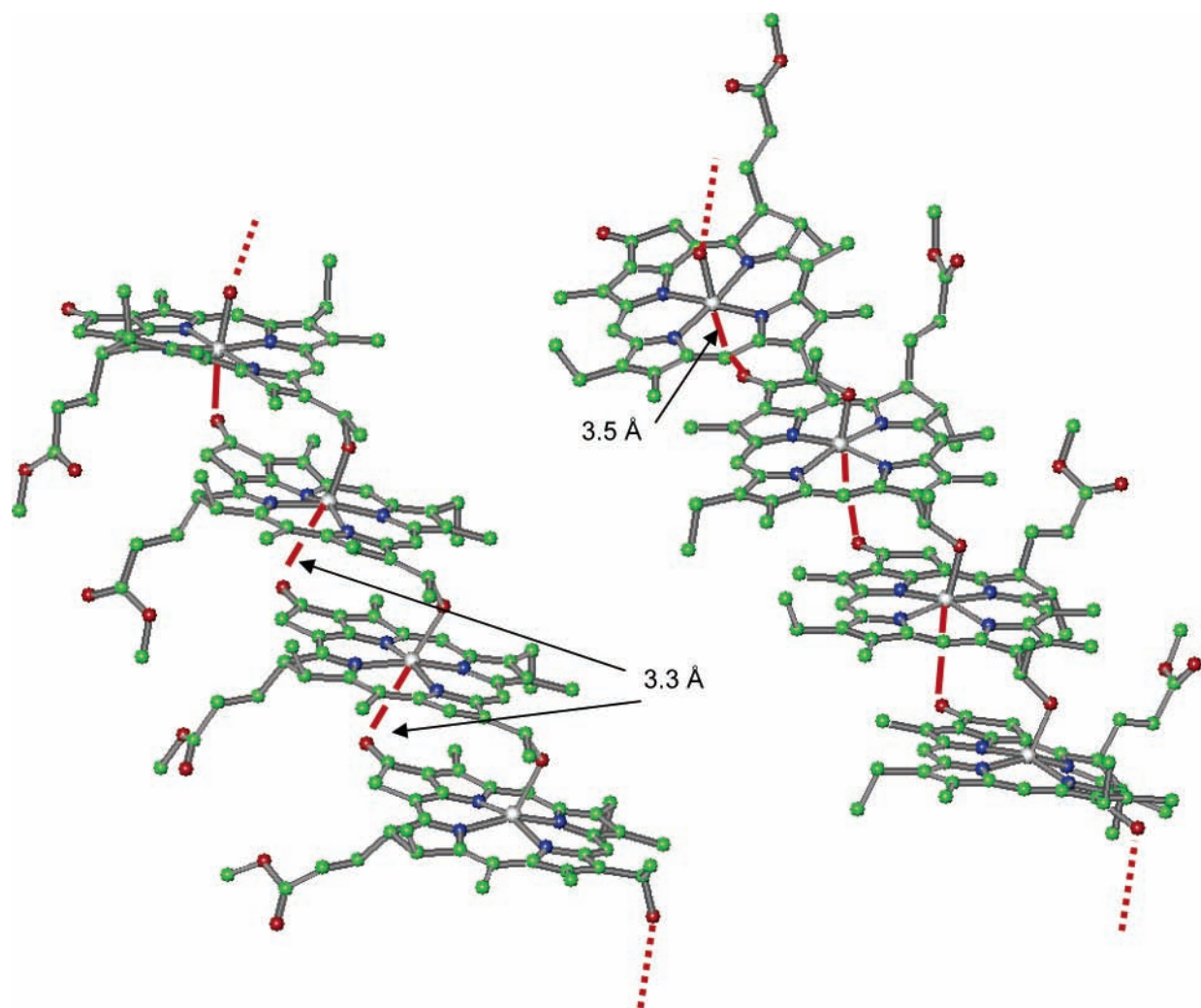


FIGURE 8. BChl *c* modeled into stacks that could pack similarly to **5** (Figure 2B). The left stack is formed exclusively of α -ligated ($3'R$)-BChl *c*, while the stack at right is β -ligated ($3'S$)-BChl *c*. In the modeled structures the farnesyl residue was replaced with a methyl group. There are several possibilities for adjacent stacks to interdigitate with average Mg–Mg distances of ~ 2 nm with either α - or β -ligations and with both *R* and *S* stereochemistries of the $3'$ carbon atom. The weak $>C=O\cdots Mg$ ligation (3.3–3.5 Å long, slightly longer than that encountered in **5**) is indicated by red lines, while the stack extension is indicated by dotted red lines. Molecular modeling was done within the HyperChem program package (Gainesville, FL).

A Novel Model for the Self-Assembly of BChl *c* within the Chlorosomes and Relevance of the Diastereotopic Ligation of Magnesium in (B)Chls

Pšenčík et al. have very recently succeeded in recording SAXS spectra and HR-TEM images of natural chlorosomes and have found a strong 2.1 nm reflex and striations along the long axis of the chlorosomes also with ~ 2 nm spacings.³¹ These authors examined all previously proposed models for the BChl *c* aggregation and found them incompatible with their data, so they proposed a novel lamellar model of antiparallel stacked BChl dimers. We agree that their strong reflexes must come from regular spacings between magnesium atoms. On the basis of knowledge on how our synthetic mimics form stacks and that the overall morphology of the self-assemblies having the racemic hydroxyethyl substituent (**5**, **6**, **8**, **10**) is astonishingly similar to that of natural chlorosomes, we are now in the unique position to propose a novel model

for the natural system. By replacing **5** in the model obtained from the crystal structure with the denser packing (Figure 2B) with BChl *c*, one obtains a lamellar structure of stacks as shown in Figure 8. As the stronger X-ray scattering atoms Zn (or Mg) are approximately in the same positions, the ~ 2 nm spacing between metal atoms in adjacent stacks is thus maintained. Figure 9 shows an artist's view of a portion of a green photosynthetic bacterium with well developed chlorosomes on the inner side of the cytoplasmic membrane. The crystal structure from the Fenna–Matthews–Olson (FMO) chlorophyll–protein complex,³² which acts as the energy trap of the BChl self-assemblies, and our model with BChl *c* forced onto the crystal packing of **5** are shown as insets. Importantly, there are two different stack configurations as the ligation of the central magnesium atom in (B)Chls is diastereotopic. In one configuration (termed α) the ligand is on the opposite side of the 17-propionic acid residue, while in the other β configuration the ligand and

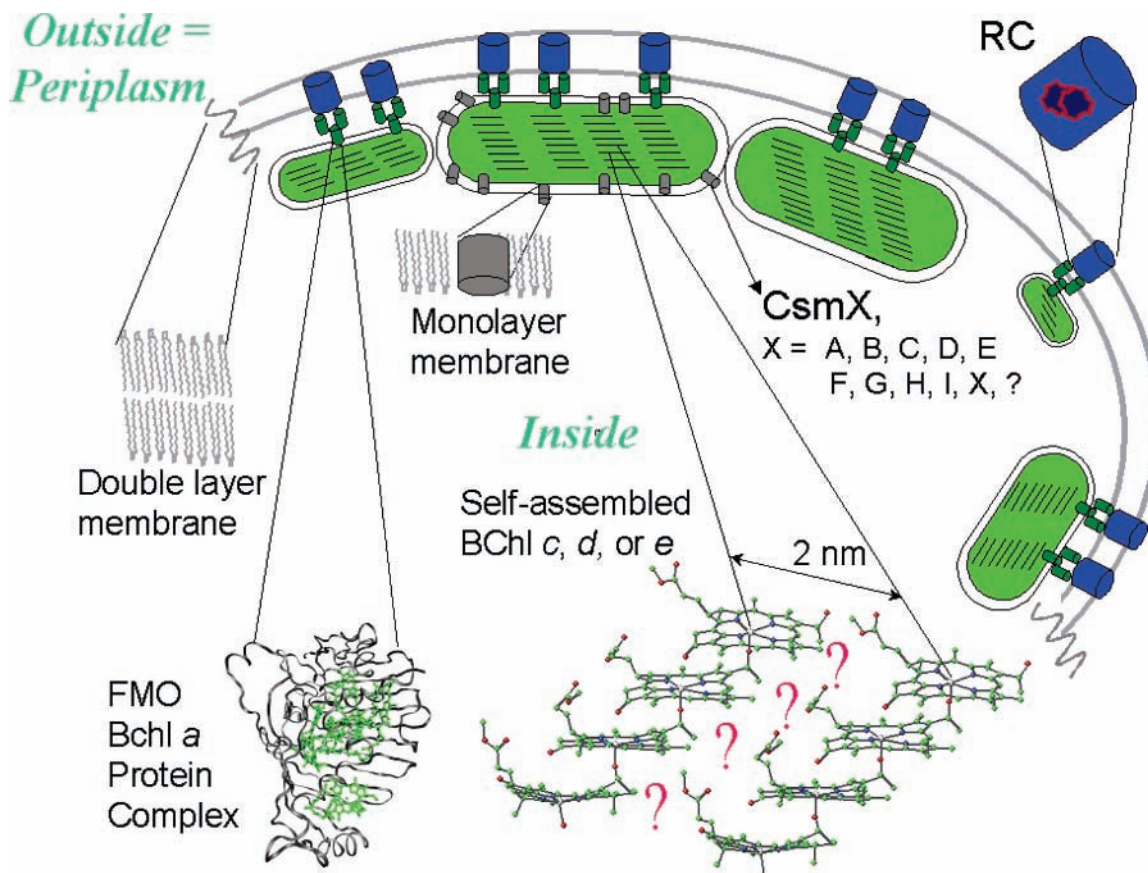


FIGURE 9. An artist's view of a portion from a green photosynthetic bacterium presenting chlorosomes. The inset in the lower left part shows the crystal structure of a monomer of the FMO protein that binds 7 BChl *a* molecules.³² The orientation of the monomer is important for the vectorial energy transfer to the reaction center (RC, shown in blue) and is not as depicted. At right is our new model for the self-assembly of BChl *c* within chlorosomes depicted as green ellipsoids. The question marks imply the yet unsolved problem whether hydrogen bonding is involved between stacks of BChls. The chlorosomes are attached to the double layer cell membrane via a baseplate that contains the chlorosomal protein CsmA. As shown by mutagenesis studies by Bryant and co-workers, all other nine known chlorosomal proteins are embedded in the monolayer lipid membrane of the chlorosome organelle and can be knocked-out without perturbing the self-assembly of BChls or the light-harvesting function of chlorosomes.^{2,48,49}

17-propionic acid residue are on the same side. Both configurations are probable, although we^{33–35} and Oba and Tamiaki³⁶ have shown that in several chlorophyll–protein complexes the α configuration is favored and that β -coordinated (B)Chls occupy specific position within the protein matrix and could be implied in the vectorial EET to the reaction center.^{33,34} Very recently, a breakthrough study by two-dimensional absorption spectroscopy brought forth experimental evidence that a β -coordinated BChl *a* gives the most red-shifted absorption out of the seven FMO BChls.³⁷

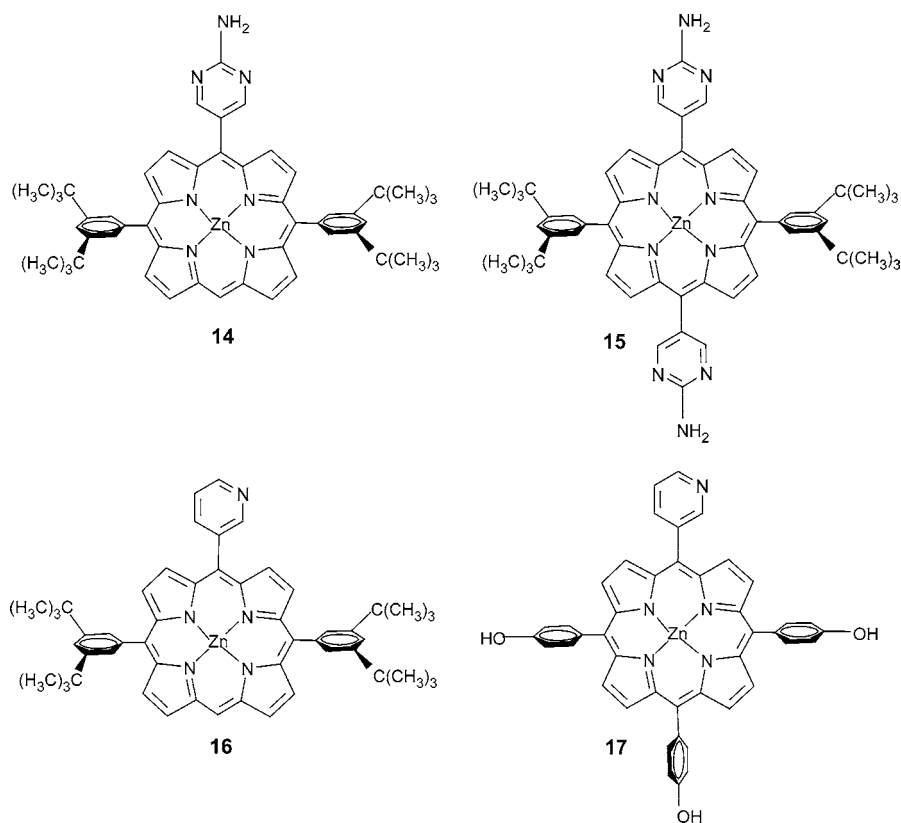
Within self-assembled BChl *c*, either in vitro or in the chlorosomes, this dichotomy has been seen as a splitting of signals in the solid-state MAS ¹³C NMR spectra of uniformly ¹³C-labeled samples.^{21,38} It remains to be confirmed if the absence of interstack hydrogen bonding is encountered also in the natural case. Because of the five-membered annulated ring, the 13-carbonyl group cannot twist out of the chlorin plane as much as the 15-acetyl group in the case of **5**. However, in the model presented here (Figures 8 and 9) the Mg \cdots O=C distance is \sim 3.3 Å and not much longer than in **5**. This might prevent the carbonyl group from being a hydrogen-bond acceptor,

despite its much lower IR frequency.²⁰ The shift to lower frequencies can be equally well explained by a weak metal ligation in the absence of any hydrogen-bonding scheme that all previous models contain. Our proposal is that the diastereotopic metal ligation with a $5^{1/2}$ coordination (4 N atoms, one strong OH ligation and a weak O=C \cdots ligation) combined with multiple hydrophobic interactions between adjacent stacks wins over putative hydrogen bonding between stacks.

Other Self-Assembly-Inducing Recognition Groups

Of course, recognition groups that can induce self-assembly other than the “natural” ones encountered in the chlorosomes as described above can be used to decorate synthetic pigments. Recently, we have proven that in the crystal structure of a similar zinc porphyrin **14** (Chart 4) equipped with a 2-aminopyrimidine recognition group, which is capable of double hydrogen bonding, hydrogen bonding can be inhibited due to encapsulation and π -stacking wins over in the interior of a porphyrinic tetramer.³⁹ The strongest supramolecular interaction is the

Chart 4



Zn-ligation by one of the two pyrimidinic nitrogen atoms. The same 2-aminopyrimidine group, but which decorates the tetramer's exterior, does engage in double hydrogen bonding, thus forming parallel strands of tetramers just as pearls are strung on a necklace (Figure 10). Due to the Zn-ligation, the other pyrimidinic nitrogen is a better hydrogen-bond acceptor, thus hierarchical and cooperative supramolecular interactions are staged. Again cyclohexane solvent molecules cement together the parallel tetrameric strands. Tetramer formation occurs also in solution, as seen from mass and absorption spectra. Due to the close approach of the porphyrin units the Soret bands are split, showing a strong excitonic coupling. Upon heating a toluene solution, the tetramers dissociate in a fully reversible manner. With two 2-aminopyrimidine groups as in **15**, oligomers are formed preferentially and not cyclic tetramers.

Presently it is difficult to "predict" the outcome of multiple supramolecular interactions, especially if many hydrophobic or dispersive forces are involved, in tailoring self-assembled architectures. The generality of this particular tetrameric porphyrinic construct is illustrated by the fact that compounds synthesized and crystallized in completely different laboratories in Japan⁴⁰ (**16**) and in Israel⁴¹ (**17**) show the same self-assembly algorithm. The 3-pyridyl group through metal ligation dictates the tetramer formation with concomitant π -stacking in the tetramer's interior. While in Tsuda and Aida's example the tetramers are not engaged in further supramolecular interactions,⁴⁰ Goldberg's tetramer,⁴¹ through the 4-phen-

olic groups, forms as in our case a hydrogen-bonding network between the tetramers.

We wish to rebuke here some criticism of supramolecular approaches stating that a crystal is not an engineered entity, as it is made of an "uncontrolled" periodic arrangement of the same single molecule. The above examples^{23,25,39–41} clearly show that supramolecules possess entirely different properties, such as broad and red-shifted absorptions and split Soret bands, than the monomers. Thus, tailoring chromophores for self-assembly⁴² consists actually in encoding into the monomer's structure the self-assembly algorithm that under appropriate conditions, such as solvent polarity and temperature, is allowed to proceed faultlessly.⁴³ Misplaced components usually have smaller binding constants, so that they can disassemble, allowing a self-repairing mechanism to operate.

Conclusion and Perspectives

The surprising finding that our self-assembling porphyrins still fluoresce in an aggregated state^{24,44} lends hope that such systems might be useful in constructing hybrid solar cells where a self-assembled antenna system is used as light-harvester for a nanostructured semiconductor. Usually concentration quenching occurs with aggregated dyes, and this has been the principal obstacle encountered in the construction of efficient solar cells that use for instance the very robust phthalocyanines. Only low IPCE values (<1%) could be obtained in such cases.⁴⁵ With our chromophores, due to the very orderly arrangement as

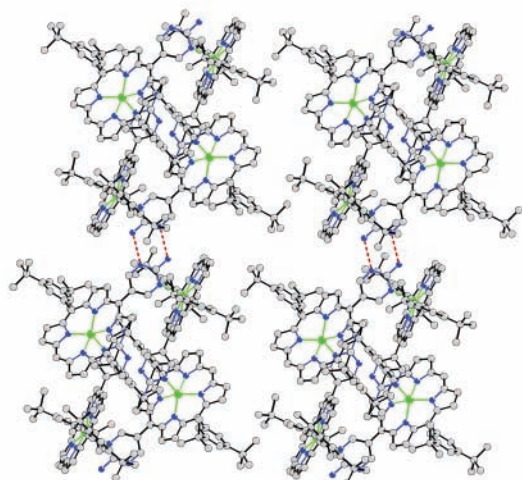
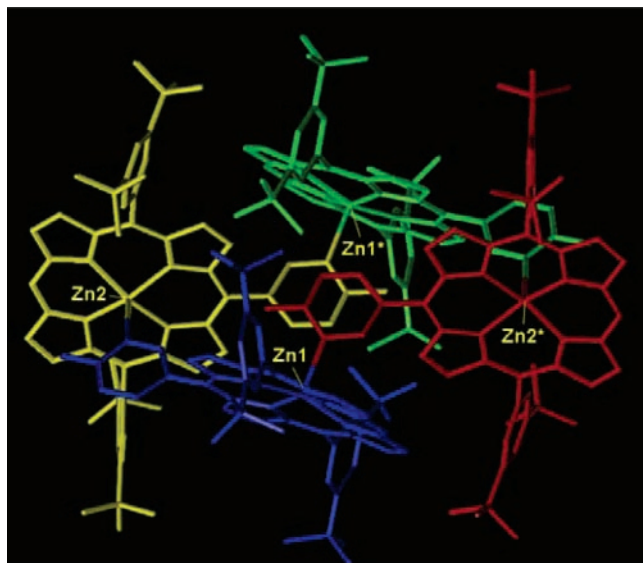


FIGURE 10. Self-assembled porphyrinic tetramers of 14 (top) and their concatenation (bottom). Solvent molecules (cyclohexane) have been omitted for clarity. Reprinted from *J. Am. Chem. Soc.* **2003**, *125*, 4233–4239. Copyright 2003 American Chemical Society.

in a protein matrix, or as has been recently shown by the group of Calzaferri, who used zeolites to organize various dye molecules,⁴⁶ concentration quenching is not operating. Very recently, by using carboxylic anchoring groups for a phthalocyanine on nanostructured titania and by preventing aggregation with axial ligands to a central ruthenium metal, a record IPCE value for phthalocyanine-sensitized solar cells of 23% at the absorption maximum could be obtained.⁴⁷

Man-made devices are often better than natural ones for performance and robustness. Typical examples are the wheels and cogwheels, for which there exists no natural counterpart, but which when coupled to an engine allow much higher velocities than any other natural joint designed for movement. However, for light-harvesting one still awaits solutions. Learning from Nature's architectural

principles might help us to devise efficient devices with robust pigments, allowing functioning at elevated temperatures (over 80 °C in the deserts), for long periods (desirable are over 20 years of serviceless functioning), or under low-light illumination conditions.

I am indebted to my wife, Carmen, for the drawings and for her support during stormy weather while allowing me to drive hard during sunny stretches, which inevitably alternate in research work on the fast lane. Prof. Jean-Marie Lehn is thanked for trusting me with common projects, as well as for his generosity, which has allowed me to pursue independent research on supramolecular ideas. In the references are mentioned the names of all the other colleagues and friends with whom I had the privilege to collaborate over the years. The experimental work in Karlsruhe was partially supported by the DFG-Center of Functional Nanostructures at the University of Karlsruhe through former projects C3.2 and C3.6 and present project C3.5.

References

- (1) Blankenship, R. E. *Molecular Mechanisms of Photosynthesis*; Blackwell: Oxford, 2002.
- (2) Balaban, T. S. Light-harvesting nanostructures. In *Encyclopedia of Nanoscience and Nanotechnology*; Nalwa, H. S., Ed.; American Scientific Publishers: Los Angeles, 2004; Vol. 4, pp 505–559.
- (3) Jordan, P.; Fromme, P.; Witt, H.-T.; Klukas, O.; Saenger, W.; Krauss, N. Three-dimensional structure of cyanobacterial Photosystem I at 2.5 Å resolution. *Nature* **2001**, *411*, 909–917.
- (4) Zouni, A.; Witt, H.-T.; Kern, J.; Fromme, P.; Krauss, N.; Saenger, W.; Orth, P. Crystal structure of Photosystem II from *Synechococcus elongatus* at 3.8 Å resolution. *Nature* **2001**, *409*, 739–743.
- (5) Brabec, C. J.; Sariciftci, N. S.; Hummelen, J. C. Plastic solar cells. *Adv. Funct. Mater.* **2001**, *11*, 15–26.
- (6) Hu, Y.-Z.; Tsukiji, S.; Shinkai, S.; Oishi, S.; Hamachi, I. Construction of artificial photosynthetic reaction centers on a protein surface: Vectorial, multistep, and proton-coupled electron transfer for long-lived charge separation. *J. Am. Chem. Soc.* **2000**, *122*, 241–253.
- (7) Li, J.; Diers, J. R.; Seth, J.; Yang, S. I.; Bocian, D. F.; Holten, D.; Lindsey, J. S. Synthesis and properties of star-shaped multiporphyrin–phthalocyanine light-harvesting arrays. *J. Org. Chem.* **1999**, *64*, 9090–9100.
- (8) Holten, D.; Bocian, D. F.; Lindsey, J. S. Probing electronic communication in covalently linked multiporphyrin arrays. A guide to the rational design of molecular photonic devices. *Acc. Chem. Res.* **2002**, *35*, 57–69.
- (9) Mongin, O.; Hoyler, N.; Gossauer, A. Synthesis and Light-Harvesting Properties of Naphaphyrins. *Eur. J. Org. Chem.* **2000**, 1193–1197.
- (10) Rucareanu, S.; Mongin, O.; Schuwey, A.; Hoyler, N.; Gossauer, A. Supramolecular assemblies between macrocyclic porphyrin hexamers and star-shaped porphyrin arrays. *J. Org. Chem.* **2001**, *66*, 4973–4988.
- (11) Hecht, S.; Fréchet, J. M. J. Dendritic Encapsulation of Function: Applying Nature's Site Isolation Principle From Biomimetics to Material Science. *Angew. Chem., Int. Ed.* **2001**, *40*, 74–91.
- (12) Lee, L. F.; Adronov, A.; Schaller, R. D.; Fréchet, J. M. J.; Saykally, R. J. Intermolecular coupling in nanometric domains of light-harvesting dendrimer films studied by photoluminescence near-field scanning optical microscopy. *J. Am. Chem. Soc.* **2003**, *125*, 536–540.
- (13) Jiang, D.-L.; Aida, T. Photoisomerization in dendrimers by harvesting of low-energy photons. *Nature* **1997**, *388*, 454–456. For a very recent contribution involving zinc porphyrin dendrimers, see: Li, W.-L.; Jiang, D.-L.; Suna, Y.; Aida, T. Cooperativity in chiroptical sensing with dendritic zinc porphyrins. *J. Am. Chem. Soc.* **2005**, *127*, 7700–7702.
- (14) Wei, T.; Reuther, E.; Müllen, K. Shape persistent, fluorescent polyphenylene dyads and a triad for efficient vectorial transduction of excitation energy. *Angew. Chem., Int. Ed.* **2002**, *41*, 1900–1904. *Angew. Chem.* **2002**, *114*, 1980–1984.
- (15) Christoffers, L. A. J.; Adronov, A.; Fréchet, J. M. J. Surface-confined light harvesting, energy transfer, and amplification of fluorescence emission in chromophore-labeled self-assembled monolayers. *Angew. Chem. Int. Ed.* **2000**, *39*, 2163–2167.

- (16) Staehelin, L. A.; Golecki, J. R.; Fuller, R. C.; Drews, G. Visualization of the supramolecular architecture of chlorosomes (Chlorobium type vesicles) in freeze-fractured cells of *Chloroflexus aurantiacus*. *Arch. Mikrobiol.* **1978**, *119*, 269–277.
- (17) Staehelin, L. A.; Golecki, J. R.; Drews, G. Supramolecular organization of Chlorosomes (Chlorobium vesicles) and their membrane attachment sites in *Chlorobium limicola*. *Biochim. Biophys. Acta* **1980**, *589*, 30–45.
- (18) Balaban, T. S.; Holzwarth, A. R.; Schaffner, K.; Boender, G.-J.; de Groot, H. J. M. CPDAS ¹³C-NMR Dipolar correlation spectroscopy of ¹³C-enriched chlorosomes and isolated bacteriochlorophyll-*c* aggregates of *Chlorobium tepidum*: The self-organization of pigments is the main structural feature of chlorosomes. *Biochemistry* **1995**, *34*, 15259–15266.
- (19) Holzwarth, A. R.; Schaffner, K. On the structure of bacteriochlorophyll molecular aggregates in the chlorosomes of green bacteria. A molecular modelling study. *Photosynth. Res.* **1994**, *41*, 225–233.
- (20) Chiefari, J.; Gribenow, K.; Fages, F.; Gribenow, N.; Balaban, T. S.; Holzwarth, A. R.; Schaffner, K. Models for the pigment organization in the chlorosomes of photosynthetic bacteria—Stereochemical control of *in-vitro* bacteriochlorophyll *c*S aggregation. *J. Phys. Chem.* **1995**, *99*, 1357–1365. Erratum. *J. Phys. Chem.* **1995**, *99*, 16194.
- (21) van Rossum, B. J.; Steensgaard, D. B.; Mulder, F. M.; Boender, G. J.; Schaffner, K.; Holzwarth, A. R.; de Groot, H. J. M. A refined model of the chlorosomal antennae of the green bacterium *Chlorobium tepidum* from proton chemical shift constraints obtained with high-field 2-D and 3-D MAS NMR dipolar correlation spectroscopy. *Biochemistry* **2001**, *40*, 1587–1595.
- (22) de Boer, I.; Matysik, J.; Amakawa, M.; Yagai, S.; Tamiaki, H.; Holzwarth, A. R.; de Groot, H. J. M. MAS NMR Structure of a microcrystalline Cd-bacteriochlorophyll *d* analogue. *J. Am. Chem. Soc.* **2003**, *125*, 13374–13375.
- (23) Balaban, T. S.; Eichhöfer, A.; Lehn, J.-M. Self-assembly by hydrogen bonding and π - π interactions in the crystal of a Porphyrin—Attempts to mimic bacteriochlorophyll *c*. *Eur. J. Org. Chem.* **2000**, 4047–4057.
- (24) Balaban, T. S.; Bhise, A. D.; Fischer, M.; Linke-Schaetzl, M.; Roussel, C.; Vanthuyne, N. Controlling chirality and optical properties of artificial antenna systems with self-assembling porphyrins. *Angew. Chem., Int. Ed.* **2003**, *42*, 2139–2144. *Angew. Chem.* **2003**, *115*, 2189–2194.
- (25) Balaban, T. S.; Linke-Schaetzl, M.; Bhise, A.; Vanthuyne, N.; Roussel, C. Green self-assembling porphyrins and chlorins as mimics of the natural bacteriochlorophylls *c*, *d* and *e*. *Eur. J. Org. Chem.* **2004**, 3919–3930.
- (26) Balaban, T. S.; Linke-Schaetzl, M.; Bhise, A. D.; Vanthuyne, N.; Roussel, C.; Anson, C. E.; Buth, G.; Eichhöfer, A.; Foster, K.; Garab, G.; Gliemann, H.; Goddard, R.; Javorfi, T.; Powell, A. K.; Rösner, H.; Schimmel, Th. Structural characterization of artificial self-assembling porphyrins that mimic the natural chlorosomal bacteriochlorophylls *c*, *d* and *e*. *Chem. Eur. J.* **2005**, *11*, 2267–2275.
- (27) Möbius, D. Scheibe aggregates. *Adv. Mater.* **1995**, *7*, 437–444.
- (28) Mishra, A.; Behera, R. K.; Behera, P. K.; Mishra, B. K.; Behera, G. M. Cyanine dyes during the 1990s: A review. *Chem. Rev.* **2000**, *100*, 1973–2012.
- (29) Balaban, T. S.; Leitich, J.; Holzwarth, A. R.; Schaffner, K. Auto-catalyzed self-aggregation of (3¹R) [Et,Et]Bacteriochlorophyll *c*F in nonpolar solvents. Analysis of the kinetics. *J. Phys. Chem. B* **2000**, *104*, 1362–1372.
- (30) Tamiaki, H.; Kimura, S.; Kimura, T. Self-aggregation of synthetic zinc 2¹-hydroxy-12¹/13¹-oxo-porphyrins. *Tetrahedron* **2003**, *59*, 7423–7435.
- (31) Pšenčík, J.; Ikonen, T. P.; Laurinmäki, P.; Merckel, M. C.; Butcher, S. J.; Serimaa, R. E.; Tuma, R. Lamellar organization of pigments in chlorosomes, the light-harvesting complexes of green photosynthetic bacteria. *Biophys. J.* **2004**, *87*, 1165–1172.
- (32) Fenna, R. E.; Matthews, B. W. Chlorophyll arrangement in a bacteriochlorophyll protein from *Chlorobium limicola*. *Nature* **1975**, *258*, 573–577. For a more recent structure from a different green bacterium, see: Li, Y.-F.; Zhou, W.; Blankenship, R. E.; Allen, J. P. Crystal structure of the bacteriochlorophyll *a* protein from *Chlorobium tepidum*. *J. Mol. Biol.* **1997**, *271*, 456–471.
- (33) Balaban, T. S.; Fromme, P.; Holzwarth, A. R.; Krauß, N.; Prokhorenko, V. I. Relevance of the diastereotopic ligation of magnesium atoms of chlorophylls of Photosystem I. *Biochim. Biophys. Acta* **2002**, *1556*, 197–207.
- (34) Balaban, T. S. Are syn ligated (bacterio)chlorophyll dimers energetic traps in light-harvesting systems? *FEBS Lett.* **2003**, *545*, 97–102. Erratum *FEBS Lett.* **2003**, *547*, 235.
- (35) Balaban, T. S. Relevance of the diastereotopic ligation of magnesium of chlorophylls in the major light-harvesting complex II (LHC II) of higher plants. *Photosynth. Res.* In press.
- (36) Oba, T.; Tamiaki, H. Which side of the π -macrocycle plane of (bacterio)chlorophylls is favored for binding the fifth ligand? *Photosynth. Res.* **2002**, *74*, 1–10.
- (37) Brixner, T.; Stenger, J.; Vaswani, H. M.; Cho, M.; Blankenship, R. E.; Fleming, G. R. Two-dimensional spectroscopy of electronic couplings in photosynthesis. *Nature* **2005**, *434*, 625–628.
- (38) van Rossum, B.-J.; van Duyl, B. Y.; Steensgaard, D. B.; Balaban, T. S.; Holzwarth, A. R.; Schaffner, K.; de Groot, H. J. M. Evidence from solid-state NMR correlation spectroscopy for two interstack arrangements in the chlorosome antenna system. In *Photosynthesis: Mechanisms and Effects*; Garab, G., Ed.; Kluwer Academic Publishers: Dordrecht, 1998; Vol I, pp 117–120.
- (39) Balaban, T. S.; Goddard, R.; Linke-Schaetzl, M.; Lehn, J.-M. 2-Aminopyrimidine directed self-assembly of zinc porphyrins containing bulky 3,5-di-*tert*-butylphenyl groups. *J. Am. Chem. Soc.* **2003**, *125*, 4233–4239.
- (40) Tsuda, A.; Sakamoto, S.; Yamaguchi, K.; Aida, T. A novel supramolecular multicolor chromophore by self-assembly of a π -extended zinc porphyrin complex. *J. Am. Chem. Soc.* **2003**, *125*, 15722–15723.
- (41) Vinodu, M.; Stein, Z.; Goldberg, I. Porphyrin supermolecules: Synthesis and self-assembly features of zinc-5-(3¹-pyridyl)-10,15,20-tris(4¹-hydroxyphenyl)porphyrin. *Inorg. Chem.* **2004**, *43*, 7582–7584.
- (42) Balaban, T. S. Synthèses, propriétés et auto-assemblage des chromophores. Habilitation, Université Louis Pasteur: Strasbourg, France, 2000.
- (43) Lehn, J.-M. *Supramolecular Chemistry, Concepts and Perspectives*; VCH: Weinheim, 1995.
- (44) Linke-Schaetzl, M.; Bhise, A. D.; Gliemann, H.; Koch, Th.; Schimmel, Th.; Balaban, T. S. Self-assembled chromophores for hybrid solar cells. *Thin Solid Films* **2004**, *451–452*, 16–21 (*Proceedings, EMRS Congress, Strasbourg, 2003*; Brabec, C. J., Saloui A., Eds.; Elsevier: Amsterdam, 2004).
- (45) He, J.; Benkő, G.; Korodi, F.; Polivka, T.; Lomoth, R.; Akermark, B.; Sun, L.; Hagfeldt, A.; Sundström, V. Modified phthalocyanines for efficient near-IR sensitization of nanostructured TiO₂ electrode. *J. Am. Chem. Soc.* **2002**, *124*, 4922–4932.
- (46) Calzaferri, G.; Huber, S.; Maas, H.; Minkowski, C. Host-guest antenna materials. *Angew. Chem., Int. Ed.* **2003**, *42*, 3732–3758. *Angew. Chem.* **2003**, *115* 3860–3888.
- (47) Yangisawa, M.; Korodi, F.; Bergquist, J.; Holmberg, A.; Hagfeldt, A.; Sun, L. Synthesis of phthalocyanines with two carboxylic acid groups and their utilization in solar cells based on nanostructured TiO₂. *J. Porphyrins Phthalocyanines* **2004**, *8*, 1228–1235.
- (48) Chung, S.; Bryant, D. A. Characterization of the *csmD* genes from *Chlorobium tepidum*. The CsmA, CsmC, CsmD, and CsmE proteins are components of the chlorosome envelope. *Photosynth. Res.* **1996**, *50*, 41–59.
- (49) Frigaard, N.-U.; Gomez Maqueo Chew, A.; Li, H.; Maresca, J. A.; Bryant, D. A. *Chlorobium tepidum*: Insights into the structure, physiology, and metabolism of a green sulfur bacterium derived from the complete genome sequence. **2003**, *78*, 93–117.

AR040211Z